Smoke reversal interaction with diagonal airway — its elusive character

J.C. Edwards, G.F. Friel, L. Yuan and R.A. Franks
Research physicist, chemical engineer, associate service fellow and electronics engineer, respectively, National Institute for Occupational Safety and Health, Pittsburgh Research Laboratory, Pittsburgh, Pennsylvania

Abstract

The reversal of smoke products-of-combustion (POC) from a mine fire was determined in a mine section with the airway connectivity of an electrical Wheatstone bridge. Four diesel-fuel fire experiments with fire heat-release rates between 504 and 771 kW were conducted in the Safety Research Coal Mine (SRCM) located at the National Institute for Occupational Safety and Health's (NIOSH) Pittsburgh Research Laboratory (PRL). Smoke reversal propagated upwind from the fire with significant leakage into the upwind diagonal airway and without causing a complete reversal of airflow in the diagonal airway. A control measure consisting of a brattice suspended half entry height from the entry roof was determined to abate the smoke rollback. Computational fluid dynamics (CFD) analysis of the smoke movement agreed with the measurements.[1]

Introduction

Diagonal airways, or connecting airways between two parallel airways, can be subjected to airflow reversal, depending on the pressure imbalances between the connected airways. As shown by Wala and Stoltz (1999), connections of diagonal airways can result in catastrophic events, such as methane explosions, if consideration is not given to the ventilation requirements. Diagonal airways are part of all mine networks and can serve useful purposes such as moving equipment from one longwall panel to another longwall panel. They also facilitate the development of mining sections by providing ventilation and access to transportation. Unlike ordinary airways to which they connect, they cannot be combined into series and parallel airways for mine ventilation planning.

The classification of airways into ordinary and diagonal airways is important for mine ventilation simulator applications. Within the local plan of a mine section, the diagonal element and the airways to which it connects form the equivalent electrical circuit of the Wheatstone bridge in which the connecting arm is the diagonal element of the ventilation circuit. From the viewpoint of graph theory, this circuit is a Hamiltonian, but not an Eulerian connected graph, because it is possible to traverse a closed path that includes every node only once but not possible to traverse a closed path that includes every airway only once. These considerations are important when determining a mesh representation for ventilation network computations.

A ventilation change induced by the movement of equipment, by the opening and closing of doors or by changes in temporary stoppings can result in airflow reversals in a diagonal airway. The diagonal airway can be unstable with respect to airflow direction because its resistance can be less than that of the airways it connects. The effect of the release of thermal energy in one of the main airways to which the diagonal airway is connected will have a more complex effect.

The thermal expansion of the POC from a fire will increase the local airway resistance, which could alter the ventilation pattern in the diagonal. Natural ventilation buoyancy forces will cause the hot POC to rise toward the mine roof and be transported with the imposed ventilation. If sufficient thermal energy is released from the fire, the momentum of the buoyant plume will be transferred at the roof into an expansion of a smoke roof layer upwind countercurrent to the imposed ventilation in the lower cross section of the entry.

Consideration in this study is given to a fire that occurs downwind from the diagonal. This smoke-laden roof layer might also migrate into the diagonal entry, and a similar countercurrent flow could result. The floor air layer can be accelerated towards the fire as the fire becomes a local low-pressure zone responsible for entraining the fresh air. The establishment of two countercurrent layers poses a challenge to predict the transport of hazardous fire POC. The problem is three dimensional, which is beyond the scope of the traditional, unidirectional flow mine-network program.

The objective of this study was to demonstrate experimentally and model with CFD the consequence of a fire in

[1] The findings and conclusions in this report are those of the authors and do not necessarily represent the views of the National Institute for Occupational Safety and Health.

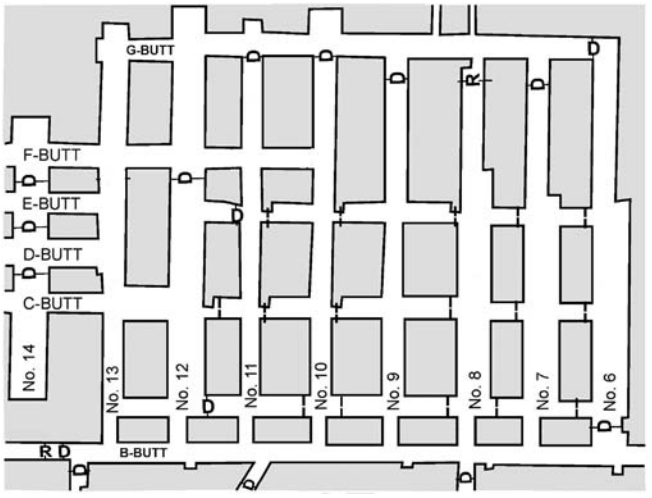

Figure 1a — Plan view of the experimental mine section in the SRCM.

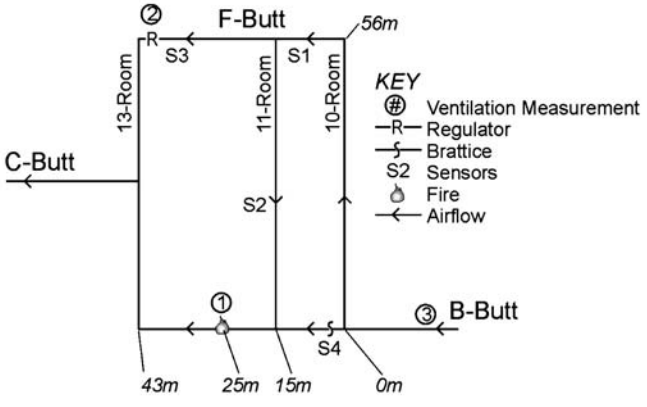

Figure 1b — Schematic diagram of the mine section for Experiments No. 1 and 2.

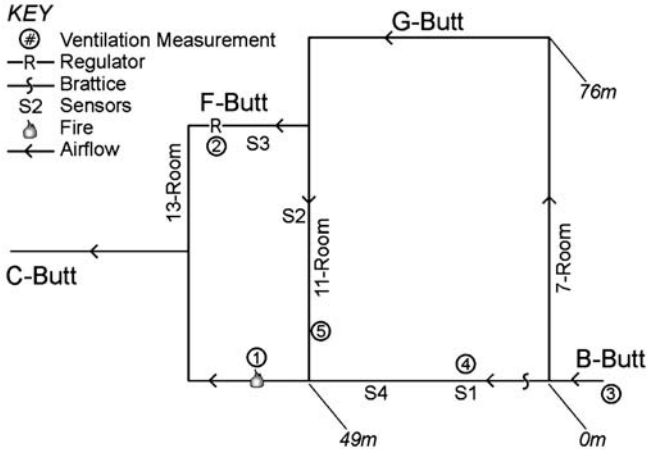

Figure 1c — Schematic diagram of the mine section for Experiments No. 3 and 4.

an intake airway downwind from a diagonal airway from the point-of-view of smoke reversal along the roof upwind in the intake and its movement into the diagonal airway. This study was based on mine fire experiments and analysis with a CFD Fire Dynamics Simulator (FDS) (McGrattan et al., 2004). FDS is a hydrodynamic simulator with chemical reactions represented by a mixture-fraction model. The effectiveness of a smoke-control measure that consists of a brattice suspended half entry height from the entry roof upwind from the fire was also determined experimentally and modeled with CFD.

Previous research (Eisner and Smith, 1954) has shown the utility of a brattice covering the lower two-thirds of the entry height as a smoke-control measure for fire fighters advancing towards a fire. This method was reported (McPherson, 1993, pp. 431 and 825) to be similar to that used for control of methane roof layers. In the case of a brattice attached to the roof and partially blocking the entry cross section there will be two effects. The first effect is to dissipate the momentum of the reverse smoke layer. As the smoke is deflected towards the floor the hot products-of-combustion (POC), momentum and energy will be through recirculation transferred to the cooler counter airflow near the floor. The second effect is the increased airflow in the open area beneath the brattice. The momentum of this airflow will push the deflected roof layer into the primary airflow towards the fire.

Experimental conditions

Four diesel-fuel-fire experiments were conducted in NIOSH's SRCM. There was no significant grade in the section of the mine in which the experiments were conducted. The mine layout plan is shown in Fig. 1a. Experiments were conducted for the air-course configurations shown in Figs. 1b and 1c. These configurations were created from the mine plan in Fig. 1a with brattices used to isolate airways. The entry heights were approximately 2 m (6.6 ft). B-Butt had an average width of 3 m (9.8 ft), whereas 11-Room and F-Butt widths were approximately 4 and 4.5 m (13 and 15 ft), respectively. The mine exhaust fan established airflow in the mine from B-Butt to F-Butt and G-Butt through connecting rooms under normal ventilation conditions. Figure 1b depicts the Wheatstone bridge ventilation circuit selected for Experiments No. 1 and 2, and Fig. 1c depicts the ventilation circuit for Experiments No. 3 and 4. 11-Room is a diagonal airway in both mine plans. It is connected to the ordinary airways B-Butt and F-Butt. The fire source was located approximately 10 m (33 ft) downwind from the center of the diagonal entry, 11-Room, for each experiment.

Regulator resistance. The selection of the fire site downwind from 11-Room required the initial reversal of the airflow from F-Butt to B-Butt in 11-Room for the purpose of determining the influence of the fire on the airflow in 11-Room. To adjust the flow so as to produce an initial low airflow from F-Butt to B-Butt in the diagonal, 11-Room, two-variable airflow resistances were introduced into the network. One variable resistance was a regulator with a sliding door constructed in F-Butt between 11-Room and 13-Room. The other variable resistance was a brattice placed across B-Butt between 10-Room and 11-Room for Experiments No. 1 and 2 and across B-Butt downwind from 7-Room for Experiments No. 3 and 4. For each experiment, the open width for the 1.60-m- (5.25-ft-) high regulator in F-Butt is listed in Table 1. The total cross-sectional dimensions in F-Butt where the regulator was constructed were 4.88 m (16.0 ft) wide and 1.88 m (6.17 ft) high.

Aerodynamic resistances for the regulator were estimated from the orifice equation for isothermal flow (Bird et al., 1960). There was significant leakage around the brattice used to regulate airflow in B-Butt along the ribs and roof. The estimated resistance for the brattice in B-Butt was based upon an airflow

balance within the mine section. The estimated resistances for the regulator and brattices used in the four experiments are listed in Table 1. The resistances for the network airways that constitute the Wheatstone bridge are less than 0.1 N s^2/m^8. The result is that the ratios of the resistances in the B-Butt segment upwind from the diagonal to the segment downwind from the diagonal are greater than 2.5, and the ratios in F- and G-Butts of the upwind to downwind segments are less than 0.2. This condition, in which the airway resistance ratio in B-Butt exceeds the airway resistance ratio in F- and G-Butts, results in a prefire airflow through the diagonal from F-Butt to B-Butt for each case based on a ventilation circuit analysis. Only if the fire provided sufficient resistance to the branch it is contained in would the airflow reverse in the diagonal. What occurs is more complex and must be considered from a three-dimensional perspective.

Table 1 — Estimated airflow resistance at F-Butt regulator and B-Butt brattice for each experiment.

Experiment No.	F-Butt regulator width, m	Regulator, N s^2/m^8	Brattice, N s^2/m^8
1	1.27	0.4	0.1
2	0.42	3.6	0.1
3	0.46	3.0	0.1
4	0.46	3.0	0.1

Ventilation. Table 2 lists the prefire airflows for each experiment at the specified locations in Figs. 1b and 1c. Airflow measurements were made with a vane anemometer for locations other than the diagonal airway. Except for the regulator, ventilation station No. 2, where a three-point measurement was made, a five-point anemometer measurement was made at each station. The five-point measurement was based on the average of the measured airflow at each of the four corners of the cross section and at the center of the cross section. The three-point measurement was based on the average of the measurements at the top, center and bottom of the open section of the regulator. In the diagonal airway at ventilation station No. 5 a smoke tube was used to estimate the airflow for experiment Nos. 3 and 4. This was based on a single time measurement near the airway center over a 3-m (10-ft) distance. For Experiments No. 1 and 2 the B-Butt airflow measurements were made upwind from the split at 10-Room, ventilation station No. 3, and for Experiments No. 3 and 4 the airflow measurement was made both upwind and downwind from the split at 7-Room at ventilation stations 3 and 4.

As expected, the volumetric airflow through the F-Butt regulator, ventilation Station No. 2, as listed in Table 2, is highest for Experiment No. 1, with the comparatively lower resistance, as shown in Table 1. Also shown in Table 2 are the predicted airflows based on an application of MFIRE (Chang et al., 1990) with the inlet airflow specified as the measured airflow at ventilation Station No. 3. The significant difference between the predicted and measured airflow values occurs at the regulator and in the diagonal airway. The discrepancy at the regulator is possibly due to leakage into F-Butt around bratticed-off cross cuts, which are connected to a parallel intake airway. The discrepancy in the diagonal is due to the inaccuracy of low airflow smoke-tube measurement.

For Experiments No. 3 and 4, the volumetric airflow at ventilation Station 5 in the diagonal based on the smoke tube measurements compared favorably with the difference between the anemometer measured airflows at ventilation Stations 1 and 4 in B-Butt. The air quantity measured with the smoke tube in the diagonal was 8.4% and 2.3% less than the difference between the anemometer measured airflows at ventilation Stations 1 and 4 in B-Butt for Experiments No. 3 and 4, respectively. Insufficient information was available to compare the diagonal airflow with F-Butt airflow.

Fire source. In the experiments the fire source on the floor in B-Butt was diesel fuel contained in two fire pans for Experiments No. 1 through 3 and a single pan for Experiment No. 4. The fire pans were approximately 8 m (26 ft) downwind from 11-Room rib. A 0.61-m- (2.0-ft-) square pan was positioned downwind from the 0.46-m- (1.5-ft-) square pan for Experiments No. 1 through 3 and a single 0.76-m- (2.5-ft-) square pan for Experiment No. 4. Table No. 3 lists the quantity of diesel fuel used for each experiment. The fuel quantities for the three experiments with two pans were proportioned according to pan area. The heat-release rate for each fire was calculated from the initial volume of diesel fuel in the pans, diesel fuel heat of combustion of 42.3 MJ/kg, fuel density of 876 kg/m^3 and fire duration based on thermocouple measurements in the fire zone. The calculated heat release rate is listed in Table 3 for each experiment.

Sensors. Figures 1b and 1c indicate the location of the sensor stations denoted by S#. The sensors at each sensor station are listed in Table 4. Sensor station S1 was located in F-Butt 5 m (16 ft) from the rib of 11-Room for Experiments No. 1 and 2. For Experiment No. 3, S1 refers to the location 33 m (108 ft)

Table 2 — Measured and predicted airflows for each experiment

Experiment No.	Location in Figs. 1b and 1c	Air velocity, m/s	Measured air quantity, m^3/s	Predicted air quantity, m^3/s	Percent error
1	1	0.68	3.26	3.11	4.6
1	2	0.91	1.84	1.14	38.0
1	3	0.96	4.26	–	–
2	1	0.60	2.84	2.58	9.1
2	2	0.78	0.52	0.32	38.5
2	3	0.65	2.89	–	–
3	1	0.76	3.58	3.83	7.1
3	2	0.79	0.58	0.48	17.2
3	3	0.95	4.31	–	–
3	4	0.49	2.16	2.19	1.4
3	5	0.15	1.30	1.64	26.1
4	1	0.70	3.29	3.54	7.6
4	2	0.87	0.64	0.44	31.2
4	3	0.88	3.99	–	–
4	4	0.49	1.98	2.02	2.0
4	5	0.15	1.28	1.52	18.7

Table 3 — Fire conditions for each experiment.

Experiment No.	Diesel fuel in 0.61-m-square pan, L	Diesel fuel in 0.46-m-square pan, L	Diesel fuel total, L	Heat release rate, kW
1	15.1	8.5	23.6	522
2	15.1	8.5	23.6	504
3	18.5	10.4	28.9	559
4	–	–	33.7	771

Table 4 — Sensors at station S# for each experiment.

Experiment No.	S1	S2	S3	S4
1	Becon	Sail, LLM1, CO15, CO17	LM	T4
2	CO7	Sail, LLM1, CO4, CO15, CO17	LM	T4
3	FloSonic, Beam	Sail, LLM1, CO4, CO15, CO17	LLM2	T4
4	–	Sail, LLM1, CO4, CO15, CO17	LLM2	T4

upwind from the fire in B-Butt. S2 included several sensors in 11-Room positioned from 16 to 28 m (52 to 92 ft) from the F-Butt rib. The location of S3 was in F-Butt approximately 2 m (6.6 ft) upwind from the regulator. Sensor Station S4 was located 13 m (43 ft) upwind from the fire. The light monitor (LM) is an incandescent light source and photocell separated by 1 m (3.3 ft) to measure the smoke obscuration. It was used at S3 for Experiments No. 1 and 2. Similarly, the laser light monitor (LLM) is a laser red light source and photocell separated by 1 m (3.3 ft). At S2 the light monitor was a laser light monitor, LLM1, and at S3 for Experiments No. 3 and 4 the light monitor was a laser light monitor, LLM2. Becon (Anglo American Research Laboratories) is an ionization smoke sensor. (Reference to a specific product is for informational purposes only and does not imply endorsement by NIOSH.) Beam (DS240, Detection Systems Inc.) is an optical smoke sensor with a transmitter and receiver separated approximately 9 m (30 ft). FloSonic (ComLink Group Inc.) is an ultrasonic airflow measurement sensor with a transmitter and receiver separated along a path similar to the Beam smoke sensor path. The carbon monoxide (CO) sensors were (Conspec Controls Inc.) diffusion mode CO sensors. In each experiment, CO17 was near the roof, and, except for Experiment No. 2, CO15 was near the floor. For Experiment No. 2, CO15 was at mid-height. The sequence of sensors at S2 in the direction from F-Butt to B-Butt consisted of CO15 and CO17, approximately 16 m (52 ft) from the F-Butt rib, followed within a 2 m (6.6 ft) distance by LLM1 and followed at another 10 m (33 ft) distance by CO4. A thermocouple, TF, was positioned in the fire pan to determine the fire duration. At S4, a thermocouple, T4, was positioned near the roof. The data were collected by an atmospheric mine monitoring system (Conspec Controls, Inc.) with a two-second data-retrieval frequency.

A triangular sail was constructed from a thin sheet of polyethylene and suspended by a nearly frictionless sharp-edged support in the lower half of the diagonal airway at S2. The cross section of the sail was normal to the longitudinal direction of the airway. Movement of the sail in the airflow was recorded by electrical contact with wires attached to the two sides of the sail. For the experiments conducted, the indicated flow was from F-Butt to B-Butt in the diagonal airway prior to each experiment. Within the duration of the experiments the flow in the lower half of the airway was maintained in opposition to the roof smoke layer that flowed from B-Butt to F-Butt.

Experimental results

Experiments No. 1 and 2. During Experiments No. 1 and 2, smoke reversal from the fire leaked around the brattice positioned across B-Butt and into 10-Room, which was approximately 15 m (50 ft) upwind from 11-Room. This smoke was visually observed to migrate along F-Butt and into 11-Room. Figure 2 shows the response of the Becon sensor for Experiment No. 1, and Fig. 3 shows the response of CO7 for Experiment No. 2 in F-Butt. The measured values of these two sensors, which were at approximately the same location in F-Butt, indicate the early arrival of the smoke from 10-Room into F-Butt. Visual observations during the experiments indicated well-mixed smoke over the 10-Room cross section. At the same time, a thick roof layer of smoke was observed visually to enter 11-Room from B-Butt as a reverse smoke roof layer. In the course of Experiments No. 1 and 2, the laser light monitor LLM1 in 11-Room and either the Becon or CO7 in F-Butt responded before CO15 and CO17 in 11-Room responded. This implies an ambiguity with regard to whether the CO17 first sensor response is to the smoke-laden roof layer that advances from B-Butt or from the smoke that advances from 10-Room. The distance between the light monitor and the vertically spaced CO sensors in 11-Room was approximately 1 m (3.3 ft) for Experiment No. 1 and 2 m (6.6 ft) for Experiments No. 2, 3 and 4. The distance between the CO sensors in 11-Room and the Becon and CO sensor in F-Butt was approximately 21 m (69 ft) for Experiments No. 1 and 2.

A comparison of Figs. 2 and 3 indicate a higher concentration at the CO sensors in 11-Room during Experiment No. 2 than during Experiment No. 1. A comparison of the light monitor normalized responses in Experiment No. 1 indicates a denser concentration of light-obscuring smoke occurred in 11-Room than reached the regulator in F-Butt. Conversely, for Experiment No. 2, more light-obscuring smoke reached the regulator than occurred in 11-Room. This is consistent with the lower airflow for Experiment No. 2, which permitted more extensive smoke reversal past the brattice in B-Butt, and its transport with the split air into 10-Room and to the regulator. The ratio of the airflow upwind from B-Butt at ventilation Station No. 3 of Experiment No. 1 to the airflow at the same location of Experiment No. 2 is 1.47. The higher volumetric airflow of Experiment No. 1 not only diluted the smoke in the reversed roof smoke layer, but also enhanced the cooling and reduced the thermally induced momentum of the reversed roof layer.

It was observed in Experiment No. 2 that the reversed smoke layer in B-Butt, which had passed around the brattice downwind from 10-Room, backed up to a doorframe in B-Butt 29 m (95 ft) upwind from the fire. The frame had a 250-mm- (10-in.-) thick roof beam across the mine entry. The roof beam stopped the movement of the smoke layer.

Experiments No. 3 and 4. Figures 4 and 5 show the POC sensors' responses for Experiments No. 3 and 4. In these experiments a longer path, approximately 50 m (165 ft) from 7-Room to 11-Room, was established for the air split to minimize the

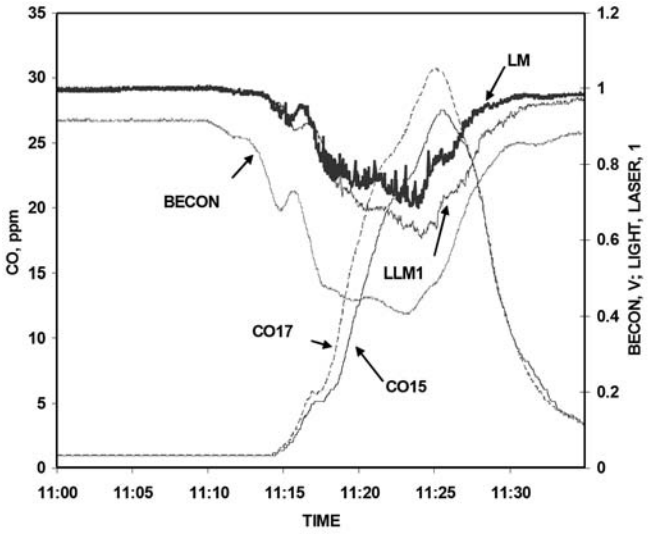

Figure 2 — Sensor measurements from Experiment No. 1.

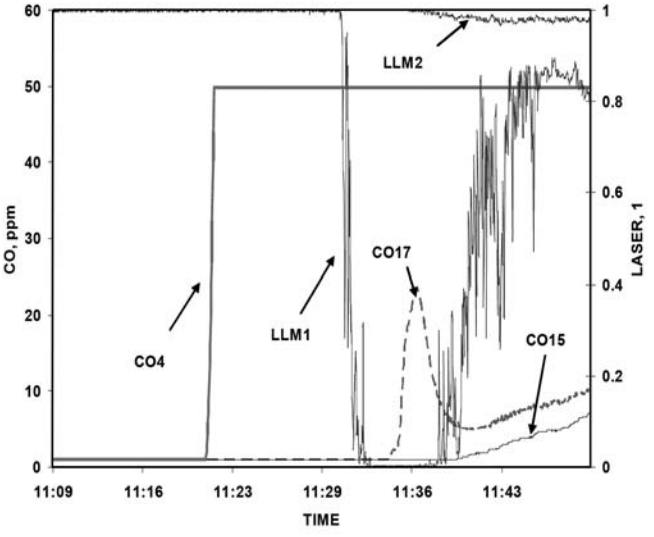

Figure 4 — Sensor measurements from Experiment No. 3.

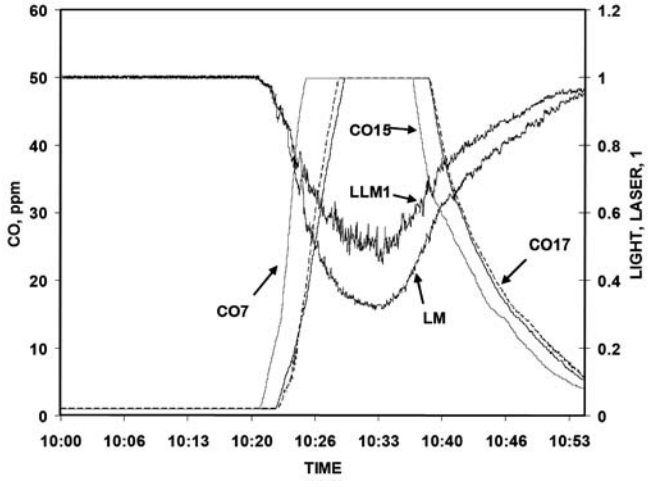

Figure 3 — Sensor measurements from Experiment No. 2.

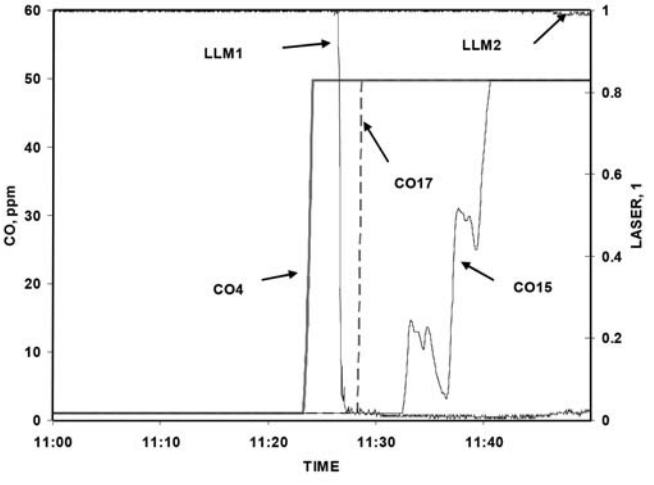

Figure 5 — Sensor measurements from Experiment No. 4.

entry of smoke from F-Butt into the diagonal from its intersection with F-Butt. Figures 4 and 5 show the reverse smoke layer in the diagonal resulted in a significantly greater response of the light monitor to smoke obscuration in the diagonal airway for Experiments No. 3 and 4 than occurred for Experiments No. 1 and 2, as shown in Figs. 2 and 3. The optical response is both more rapid and indicates total obscuration instead of the partial obscuration that occurred in Experiments No. 1 and 2. This difference in smoke intensity is the result of the more intense heat production for Experiments No. 3 and 4 than for Experiments No. 1 and 2, as shown in Table 3.

Another difference in sensor response between Experiments No. 1 and 2 and Experiments No. 3 and 4 is the response of CO sensors CO17 and CO15. For Experiments No. 1 and 2, CO15 and CO17 in the diagonal airway responded simultaneously. The CO sensor responses would indicate the smoke laden air from 10-Room, which was observed to be well mixed, had reached the 11-Room CO sensors at approximately the same time as the reversed smoke layer in 11-Room. This is to be contrasted with Experiments No. 3 and 4, which indicate a lag in the time of arrival at the roof and floor CO sensors. For these latter two experiments, the inability of the smoke roof layer to travel to the upwind split at 7-Room precluded smoke entering 11-Room from F-Butt.

In Experiment No. 3, CO sensor No. 17 indicated a first response at 11:35 am. This time corresponds to the initiation of the decrease in the fire intensity as interpreted by a reduction in the thermocouple temperature in the fire zone above the large pan. When CO17 reached a maximum, the temperature in the fire zone has decreased to 325°C (620°F). It was visually observed in B-Butt that the smoke layer commenced to retreat about 11:33 am, which is also characteristic of decreasing fire intensity. For Experiments No. 1, 2 and 4, the CO sensor response in 11-Room occurred in the steady state period of the diesel fuel burn. This can be attributed to the higher airflow in the fire zone for Experiment No. 3 relative to the other three experiments.

Unlike Experiment No. 2, in Experiment No. 3 with 10-Room isolated with brattices at the B-Butt and F-Butt ends, the smoke was only temporarily stopped by the doorframe in B-Butt. The layer thickened vertically below the beam and formed a recirculation zone below the roof before advancing

Figure 6 — Brattice blockage of smoke 29 m (95 ft) upwind from the fire in B-Butt in Experiment No. 4.

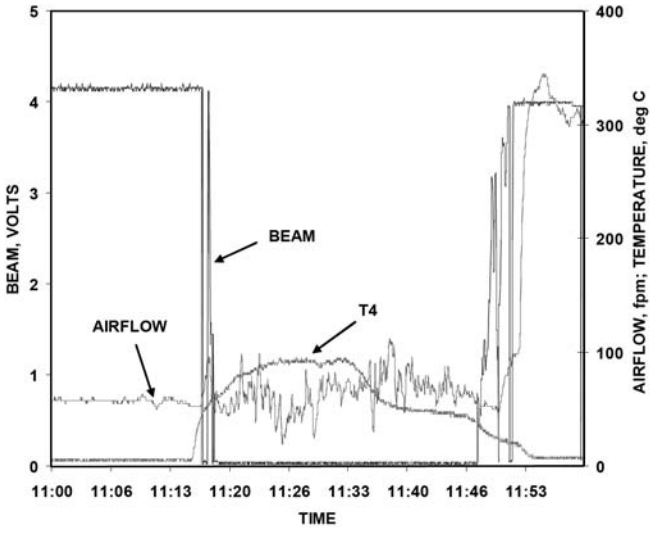

Figure 7 — Sensor response in B-Butt from Experiment No. 3.

farther upwind from the doorframe. The smoke advanced 10 m (33 ft) upwind from the doorframe. The average airflow velocity between the fire and the extent of the reverse layer can be estimated from the measured air velocities at the fire zone and upwind from the diagonal air split. That average velocity is 0.55 m/s (1.8 fps). Based on earlier research (Edwards et al., 2006), the estimated critical air velocity required to prevent reverse smoke layer would be 1.96 m/s (6.4 fps).

Based on the observation of the temporary stoppage of smoke by the doorframe located 29 m (95 ft) upwind from the fire in Experiment No. 3, Experiment No. 4 was conducted with a brattice secured tightly along the roof and ribs of the doorframe and extending 0.91 m (3.0 ft) down from the roof. The brattice was set in place prior to the airflow measurements. The doorframe dimensions were 1.75 m (5.74 ft) high and 2.51 m (8.23 ft) wide. It was observed during the experiment that a roof smoke layer retreated upwind with an approximate speed of 0.19 m/s (0.62 fps) until it reached the partial brattice covering at the door frame. This was counter to the average airflow of 0.55 m/s (1.8 fps) between the fire and the upwind brattice. Based on previous research (Edwards et al., 2006), the critical velocity to prevent smoke rollback would be 2.1 m/s (6.9 fps) for the 771 kW fire, which is greater than the 0.55 m/s (1.8 fps) in the entry. The smoke layer's reversal was blocked by the brattice. It was observed that the smoke recirculation extended less than 0.3 m (1 ft) beneath the bottom of the brattice. Figure 6 shows the brattice and the smoke slightly below the brattice.

For all four experiments the light monitor in F-Butt between the regulators and 11-Room responded to smoke. An initial advancement of a smoke roof layer was visually observed in 13-Room slightly beyond C-Butt and toward G-Butt for Experiment No. 1. The relatively small response of the light monitor upwind from the regulator in F-Butt for Experiments No. 3 and 4 compared with Experiments No. 1 and 2 indicates that the significant responses in the first two experiments were due to smoke leakage from 10-Room into F-butt. This illustrates the elusive characteristic of smoke when temperature induced buoyancy effects compete with forced ventilation.

The buoyancy effect in the reversed smoke layer is seen in the temperature near the roof in B-Butt 15 m (50 ft) upwind from the fire for Experiment No. 3, as shown in Fig. 7. The smoke temperature reaches a temperature of 95°C (200°F), which is significantly higher than the ambient air temperature of 4°C (39°F). Also shown in Fig. 7 are the responses of the Beam optical smoke sensor and FloSonic ultrasonic airflow monitor in B-Butt 9 m (30 ft) upwind from the fire. The response of the Beam optical smoke sensor is coincident with the increase in fluctuations of the FloSonic airflow monitor. These fluctuations in the acoustic velocity monitor are due to the refraction and absorption of ultrasound waves by the smoke-laden air. This effect was discussed in a previous study (Friel and Edwards, 1996) on the acoustic detection of smoke from a fire.

CFD modeling

CFD modeling can be used to determine the smoke movement, concentration and temperature produced by a fire in a mine entry. CFD requires a specification of the mine dimensions, inlet airflows and fire intensity. The three-dimensional character of a CFD application yields a prediction of the extent of smoke reversal directly upwind from the fire and into a diagonal airway that intersects the airway with the fire. Nonuniform pressure imbalances between the ends of the diagonal airway can result in partial airflow reversals. This is not available from standard mine ventilation simulators for unidirectional airflow. The spatial resolution required for CFD three-dimensional modeling imposes practical limitations on the extent of the mine section that can be modeled. These limitations are determined by the computer memory and processor speed. Implicit in the FDS, the CFD program used in this study is a rigorous treatment of the throttling and acceleration effects imposed by a fire upon the airflow. Beyond the application of FDS to a localized mine section, a standard mine ventilation simulator can provide information on the spread of smoke and heat to the remainder of a mine if the smoke is well mixed over the mine entry. This suggests a coupling of the output from a CFD application to the input of a mine ventilation simulator to model the entire mine.

FDS analysis was applied to model the smoke (soot) concentration and airflow in the entries and connecting rooms. For Experiment No. 2, Fig. 8 is a plan view that shows the predicted smoke concentration 200 mm (8 in.) below the roof, and Fig. 9 is a profile view of the predicted smoke distribution. Figure 8 shows the reversed smoke layer that advanced

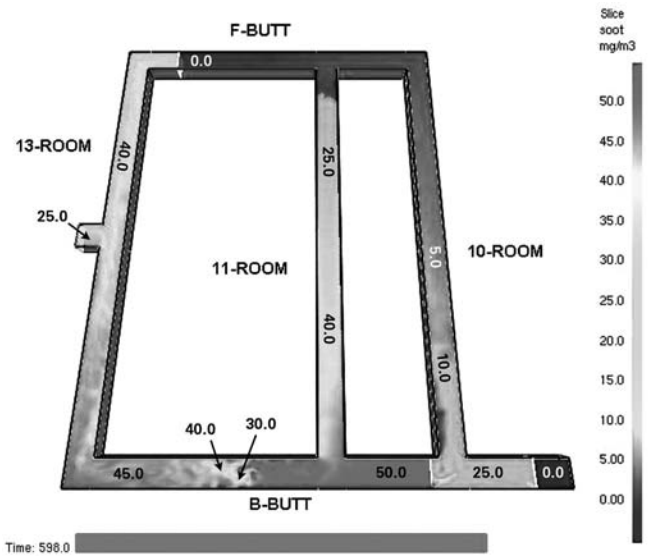

Figure 8 — Predicted smoke density 200 mm (8 in.) below roof in Experiment No. 2.

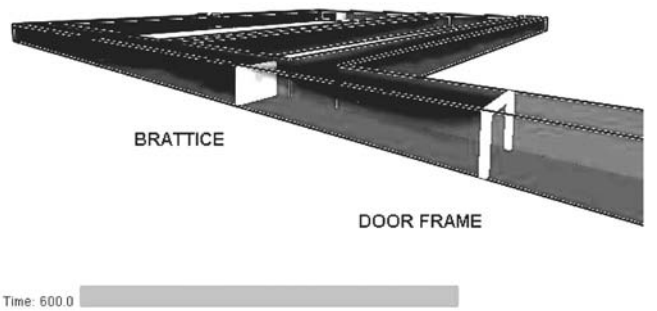

Figure 9 — Predicted smoke density abatement by the doorframe in Experiment No. 2.

Figure 10 — FDS simulation of smoke blockage by the partial brattice in Experiment No. 4.

into both 10-Room and 11-Room. The predicted smoke (soot) concentration in Fig. 8 is in units of mg/m^3. The CFD prediction of the smoke distribution shown in Fig. 8 is in agreement with the experimental observation for the smoke abatement in Experiment No. 2 at the B-Butt doorframe.

An application of FDS was made to Experiment No. 3 to model the smoke reversal in B-Butt. FDS computations showed a temporary smoke stoppage, but the predicted smoke movement was approximately 30 m (100 ft) upwind from the doorframe. The experimental observation was 10 m (33 ft) of smoke advancement upwind from the doorframe.

The effectiveness of the blockage of smoke reversal by the brattice suspended from the roof in B-Butt during Experiment No. 4 was modeled with the FDS program. The result of the simulation is shown in Fig. 10. Although the simulation showed a small amount of leakage upwind underneath the brattice, which was not observed in the experiment, the smoke reversal was essentially blocked.

An FDS application to Experiment No. 4 was used to predict the airflow and smoke density in the diagonal airway. Figure 11 shows the smoke concentrations and airflow directions along a middle vertical plane parallel to the direction of the diagonal airway. The arrows indicate the airflow direction. The location Y = 0 m is the location of the B-Butt rib and Y = 53 m (175 ft) is the location of the F-Butt rib. In the upper section the figure shows the roof smoke-layer movement from B-Butt to F-Butt, and the lower section shows the airflow movement from F-Butt to B-Butt. The smoke concentrations indicated by the contour lines are not actual concentrations but only relative concentrations. As expected, the denser smoke concentration occurs near the roof closer to B-Butt. This is in qualitative agreement with the CO concentration reported in Fig. 5, which shows higher CO concentration near the roof than near the floor. The CO concentrations in Fig. 5 are eventually truncated by the maximum measurable value of 50 ppm.

During Experiment No. 4, the response of the thermocouple in the fire, TF, and the thermocouple, T4, 13 m (43 ft) upwind from the fire in B-Butt are shown in Fig. 12 along with the values predicted by the FDS program. The CFD simulation was terminated after a steady state was achieved. The predicted temperature upwind from the fire was in relatively good agreement with the measured temperature. Temperature prediction within the fire is affected by the reaction kinetics of the fire. In the simulation the heat production is specified in the fire zone, which would result in more accurate temperature prediction away from the heat source. One significant difference between the measurement and the simulation was the time for the hot gases in the reversed smoke layer to reach the upwind thermocouple T4. The measured temperature increase at T4 occurred 80 seconds after ignition of the fire, whereas the predicted value was reached 16 seconds after ignition. This was a consequence of the treatment of turbulence by FDS. The FDS does not account for the mine wall friction, which would retard the advancement of the reversed smoke layer. An earlier response of the predicted value in comparison with the measured value was also seen in the response of the laser light monitor LLM1 in 11-Room. The laser light monitor responded to smoke 7 min after the initiation of the fire. However, the FDS predicted a response about 2.4 min after initiation of the fire. There was a roof cavity with a depth near to but less than 1 m (3.3 ft) in 11-Room between B-Butt and the laser light monitor, which would have retarded the advancement of the reversed roof smoke layer in 11-Room.

Conclusions

How smoke from a mine fire downwind from a diagonal airway can undergo reversal into the diagonal airway without causing a complete airflow reversal in the airway was demonstrated experimentally and modeled successfully with a CFD program. For fire intensities between 504 and 771 kW complete flow reversal did not occur in the diagonal airway. Instead of a total airflow reversal in the diagonal airway, the roof smoke layer flowed counter to the established airflow along the floor. A

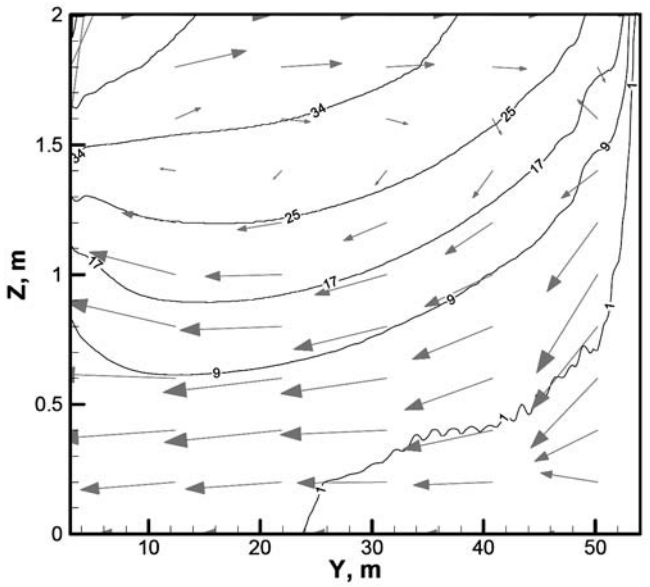

Figure 11 — Predicted airflow direction and smoke concentration (mg/m^3) along the middle, vertical plane parallel to the direction of the diagonal airway in Experiment No. 4.

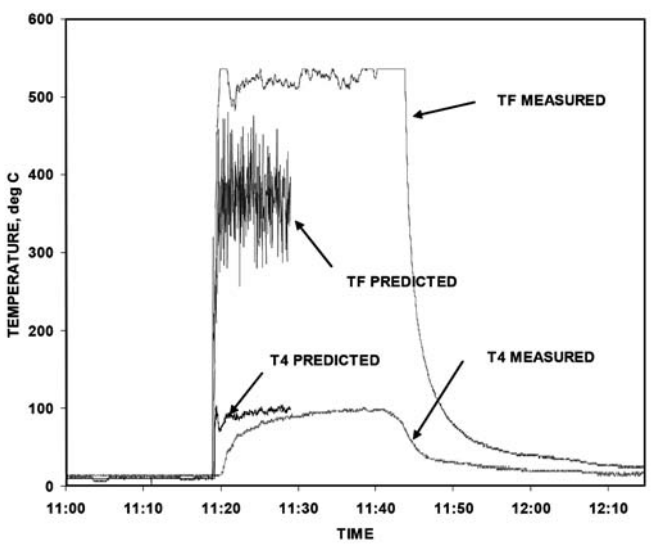

Figure 12 — Measured and predicted temperatures in fire and near the roof 13 m (43 ft) upwind from the fire in B-Butt in Experiment No. 4.

smoke reverse layer extended 8 m (26 ft) upwind from the fire to the diagonal and at least 40 m (130 ft) along the diagonal counter to the established airflow, as determined by the CO sensors in the diagonal. This event in a simple mine airway configuration is not modeled by standard mine-ventilation network simulators, which are dependent on unidirectional airflow in any particular airway. Preventive planning with recommendations for miner egress and rescue are complicated by the smoke reversal into connecting airways. CFD analysis is a viable method to predict the formation of reversed smoke layers, and their movement provided the input parameters, such as mine dimensions, airflow quantities and fire intensity, are sufficiently known.

It was demonstrated for a 771-kW fire that smoke reversal could be abated by a partial brattice coverage extending from the roof to approximately half the entry height. The 29 m (95 ft) distance of the brattice from the fire zone would make the ventilation effect localized. This is a possible smoke-reversal control measure for mine rescue. The FDS program was shown to be useful for determining the extent of fire-generated, roof-smoke reversal and the abatement of the smoke by a brattice suspended from the roof to mid-height. The turbulence model in FDS did not adequately account for the rate of roof smoke reversal. Additional research on the implementation of CFD methods needs to be conducted for a variety of conditions, which include airway dimensions, brattice cross-sectional area restriction, fire intensity and airflow. For each mine-entry configuration and partial entry blockage with a brattice, a critical ventilation velocity can be determined as a function of fire intensity which prevents smoke reversal. Given the complexities for conducting the experiments, a limited number of experiments could be modeled with a CFD application. Based on a successful comparison of predictions with experimental results, additional CFD applications could be used to determine a more comprehensive relationship between critical velocities, fire intensity, airway dimensions and smoke-control measures. The experimental problem encountered in determining if the smoke arrival in the diagonal airway near the F-Butt airway was from the smoke reversed layer in the diagonal or from 10-Room could be resolved with additional POC monitoring in the diagonal. This should be incorporated in future research.

As a subsidiary measurement, it was further demonstrated how an ultrasonic path airflow monitor can detect smoke from a mine fire by its erratic fluctuations. These fluctuations in the signal are caused by the attenuation and refraction of sound waves by smoke particulates in the airflow.

Acknowledgment

The authors acknowledge Paul Stefko, Joseph Sabo and Jack Teatino, who maintain the SRCM at the PRL, for their assistance in preparation of the experiments.

References

Bird, R.B., Stewart, W.E., and Lightfoot, E.N., 1960, *Transport Phenomena*, J. Wiley & Sons, Inc., New York, p. 226.

Chang, X., Laage, L.W., and Greuer, R.E., 1990, "A User's Manual for MFIRE: A Computer Simulation Program for Mine Ventilation and Fire Modeling," U.S. Bureau of Mines Informational Circular 9245, 171 pages.

Edwards, J.C., Franks, R.A., Friel, G.F., and Yuan, L., 2006, "Experimental and modeling investigation of the effect of ventilation on smoke rollback in a mine entry," *Mining Engineering*, April 2006, pp. 53-58.

Eisner, H.S., and Smith, P.B., 1954, "Convection Effects from Underground Fires: The Backing of Smoke Against the Ventilation," Safety in Mines Research Establishment Report No. 96, 12 p. July

Friel, G.F., and Edwards, J.C., 1996, "Mine Fire Detection by Ultrasonic Ranging Systems," U.S. Bureau of Mines RI 9624, 15 pages.

McGrattan, K.B., Forney, G.P., Floyd, J.E., Hostikka, S., and Prasad, K., 2004, Fire Dynamics Simulator (Version 4) User's Guide, U.S. Dept. of Commerce, National Institute of Standards and Technology, NIST Special Publication 1019, U.S. Government Printing Office, Washington, D.C., July

McPherson, M.J., 1993, *Subsurface Ventilation and Environmental Engineering*, Chapman and Hall, New York, 905 pp.

Wala, A.M., and Stoltz, J.R., 1999, "Three underground coal mine explosions — twenty miners killed — one reason," *Proceedings of the 8th US Mine Ventilation Symposium*, J. Tien, ed., Univ. of Missouri-Rolla Press, Rolla, Missouri, pp. 397-404, June 11-17, 1999.